Study on Frequency Synchronization in 3GPP LTE System for FDD and TDD Modes*

Meilin Wang, Xin Qi, Limin Xiao, Min Huang, and Ming Zhao

Tsinghua National Laboratory for Information Science and Technology,
Tsinghua University, Beijing, P.R. China
meilinwang@126.com

Abstract. In this paper, we propose a novel frequency synchronization method in 3GPP long term evolution (LTE) system downlink for both frequency division duplex (FDD) and time division duplex (TDD) modes. The proposed method includes coarse frequency offset estimation (FOE) using primary synchronization signal (PSS) based correlation in time domain, and fine FOE using phase difference between PSS and secondary synchronization signal (SSS) in frequency domain. Traditionally, cyclic prefix (CP) based method is widely used for fine FOE which is however sensitive to the time synchronization error and multi-path fading channel environment. The proposed fine FOE shows an apparent advantage in both FDD and TDD modes compared with CP based method. In addition, both theoretical analysis and simulation results show that the proposed fine FOE in TDD mode outperforms that in FDD mode under the same system assumptions. The simulations are done under a dual-cell scenario where there is co-frequency interference from the adjacent cell.

Keywords: 3GPP LTE, cell search, dual-cell, frequency synchronization.

1 Introduction

The 3GPP long term evolution (LTE) is acknowledged as one of the dominant technologies for next-generation wireless cellular communication systems, which can provide wide bandwidth access and high data-rate throughput of exceeding 100Mbps in downlink and 50Mbps in uplink, as well as lower latency with round-trip-time of less than 10ms. LTE supports both frequency division duplex (FDD) mode and time division duplex (TDD) mode, as well as frequency flexibility with from 1.4MHz to 20MHz allocations.

The multiple access scheme in LTE downlink employs orthogonal frequency division multiple access (OFDMA) in downlink and single carrier frequency division multiple access (SC-FDMA) in uplink [1]. These solutions provide orthogonality between the users, reducing the interference and improving the network capacity.

* This work was supported by National Basic Research Program of China (2007CB310608), National Natural Science Foundation of China (60832008), China's 863 Project (2009AA011501), National S&T Major Project (2009ZX03002-002), NCET and PCSIRT.

P. Ren et al. (Eds.): WICON 2011, LNICST 98, pp. 180–191, 2012.

However, Carrier frequency offset (CFO) introduces interference among sub-carriers and deteriorate the system performance. To overcome the imperfection, tight frequency synchronization is required.

The frequency synchronization of LTE system usually requires two steps: coarse frequency offset estimation (FOE) and fine FOE. Coarse FOE is used to reduce the frequency error within a certain range, then fine FOE is applied to make a finer correction and track further frequency shifting after initial synchronization is done. Traditionally, primary synchronization signal (PSS) or secondary synchronization signal (SSS) based cross-correlation in frequency domain is widely used for coarse FOE to estimate the integer part of CFO, and cyclic prefix (CP) based autocorrelation is applied for fine FOE to estimate the fractional part [2][3]. However, in the multi-path channel environment, CP based method suffers from performance degradation, especially in the practical multi-cell scenario. Though the performance can be improved by increasing the number of OFDM symbols in the CP autocorrelation, the computational complexity is increased greatly as well. Moreover, in TDD mode, there is no signal in uplink subframes, so extra effort should be taken in the tracking loop, e.g. adding an uplink-downlink switch to stop tracking residual CFO during the uplink subframe duration [4].

In this paper, we propose a frequency synchronization method including coarse FOE based on PSS and fine FOE jointly based on PSS and SSS. The proposed fine FOE executed in frequency domain can combat the multi-path channel more effectively and obtain better performance compared with CP based method. In FDD and TDD modes, the gaps between the PSS and SSS have different lengths, which leads to that the proposed FOE using the phase difference has different detecting ranges and estimation accuracies. The simulation results show that the proposed fine FOE in TDD could estimate the CFO more accurately but may need higher computational complexity in coarse FOE than that in FDD.

2 LTE Synchronization Overview

LTE defines two radio frame structures, i.e. Type1 and Type2 which are applicable to FDD mode and TDD mode respectively [5]. One radio frame has 10 ms duration and consists of 10 subframes, each with two consecutive slots. Hierarchical synchronization signals including PSS and SSS are designed for the purpose of setting up downlink synchronization between the E-UTRAN NodeB (eNB) and the User Equipment (UE) in LTE system. There are 504 unique physical-layer cell identities. The physical-layer cell identities are grouped into 168 unique physical-layer cell-identity groups represented by $N_{\mathrm{ID}}^{(1)}$ (from 0 to 167), each group containing three unique identities represented by $N_{\mathrm{ID}}^{(2)}$ (from 0 to 2), thus the cell identity is uniquely determined by $N_{\mathrm{ID}}^{\mathrm{cell}} = 3N_{\mathrm{ID}}^{(1)} + N_{\mathrm{ID}}^{(2)}$. As shown in Fig. 1, in time domain, PSS and SSS are transmitted periodically, twice per 10ms. SSS is transmitted in the symbol immediately preceding PSS in FDD mode, while 3 OFDM symbols ahead of PSS in TDD mode. In both modes, PSS and SSS are transmitted in the central 6 resource blocks (RBs) in frequency domain, which is independent to the system bandwidth. More specifically, PSS and SSS are both 62-point sequences mapped to the central 62 resource elements (REs) with 5 REs guarded at each of the two sides of frequency domain.

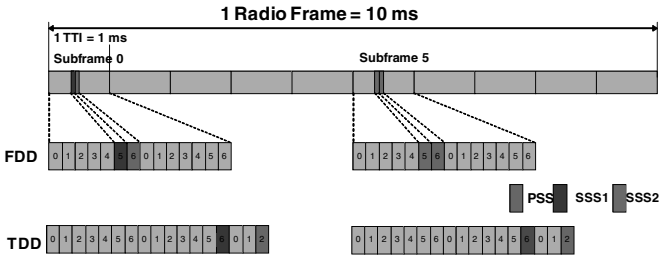

Fig. 1. PSS and SSS locations in FDD and TDD Frame structures

2.1 PSS Sequence

The sequence $d(n)$ used for the PSS is generated from a frequency-domain Zadoff-Chu sequence according to

$$d_u(n) = \begin{cases} e^{-j\frac{\pi un(n+1)}{63}} & n = 0,1,...,30 \\ e^{-j\frac{\pi u(n+1)(n+2)}{63}} & n = 31,32,...,61 \end{cases} . \tag{1}$$

where the Zadoff-Chu root sequence index μ can be 25, 29,34 corresponding to $N_{\mathrm{ID}}^{(2)}$ equaling to 0, 1, 2 respectively.

2.2 SSS Sequence

SSS is a length-62 frequency-domain sequence $q(n)$ which is an interleaved concatenation of two 31-bit binary M-sequences $s_0(n)$ and $s_1(n)$ with cyclic shifts dependent on a pair of integers, m_0 and m_1, which are uniquely determined by $N_{\mathrm{ID}}^{(1)}$. In order to distinguish between the cells within a cell group and reduce the peak to average power ratio (PAPR), both sequences are scrambled with one of two M-sequence $c_0(n)$ or $c_1(n)$, which are cyclic shift versions of $\tilde{c}(n)$ determined by $N_{\mathrm{ID}}^{(2)}$. Moreover the even sequence is scrambled with one of another two scrambling sequences $z_1^{(m_0)}(n)$ and $z_1^{(m_1)}(n)$ which are defined by two cyclic shifts of the M-sequence $\tilde{z}(n)$. The combination of two length-31 sequences defining the SSS differs between subframe 0 and subframe 5 according to

$$\begin{aligned} q(2n) &= \begin{cases} s_0^{(m_0)}(n)c_0(n) & \text{in subframe 0} \\ s_1^{(m_1)}(n)c_0(n) & \text{in subframe 5} \end{cases} \\ q(2n+1) &= \begin{cases} s_1^{(m_1)}(n)c_1(n)z_1^{(m_0)}(n) & \text{in subframe 0} \\ s_0^{(m_0)}(n)c_1(n)z_1^{(m_1)}(n) & \text{in subframe 5} \end{cases} \end{aligned} . \tag{2}$$

2.3 Overall Initial Cell Search Procedure

When a UE accesses to LTE cellular network, it needs to establish synchronous connection as fast as possible with the best serving eNB. According to synchronization signals and frame structure, the initial cell search procedure can be divided into 3 steps. Firstly, cross-correlation between the received signal and 3 local PSS replicas in time domain has to be done on different available carrier frequencies to identify the serving carrier frequency. Once it succeeds, symbol timing, half-frame timing, as well as PSS identity $N_{\mathrm{ID}}^{(2)}$ are acquired. Secondly, SSS detection is executed to obtain the SSS identity $N_{\mathrm{ID}}^{(1)}$ and the frame timing. Since CFO has severe impact on the performance of SSS searching, coarse FOE is needed before SSS detection. The last step is the fine FOE which estimates and compensates residual frequency error.

3 Frequency Synchronization

3.1 System Model

In LTE cellular network, we suppose all the cells operate at the same frequency carrier. Let $\mathrm{eNB_i}$ denote the i-th eNB. In downlink, each $\mathrm{eNB_i}$ generates a serial discrete baseband OFDM sample stream $s_i(n)$; Transmitting over multi-path fading channel under consideration of a carrier frequency misalignment Δf_i between transmitter and receiver as well as gaussian noise $w(n)$, the received signal $r(n)$ at UE will be

$$r(n) = \sum_i (s_i(n) \otimes h_i(n,l)) e^{j2\pi \Delta f_i n T_s} + w(n) \quad . \tag{3}$$

where $h(n,l)$ denotes the time-variant channel impulse response for the l-th OFDM symbol, T_s denotes the system sampling period, $\otimes$ stands for the linear convolution.

3.2 FOE Algorithm

In this paper, a two-step FOE method including coarse FOE done in time domain using PSS, and fine FOE done in frequency domain using both PSS and SSS is applied. Before fine FOE, coarse FOE is needed to compensate the initial CFO, so that the residual CFO is within the fine FOE detectable range.

The proposed coarse FOE is performed in time domain with local replica of PSS sequence based correlation. The sequence $p(l)$, i.e. IDFT of the sequence $d(n)$ defined in (1), is given by

$$p(l) = \sum_{n=1}^{31} d(n+30) e^{j\frac{2\pi nl}{N_s}} + \sum_{n=N_s-31}^{N_s-1} d(n-N_s+31) e^{j\frac{2\pi nl}{N_s}}, 0 \le l \le N_s - 1 \quad . \tag{4}$$

where the IDFT size N_s is determined by the sampling rate of the received data, e.g. for 20MHz-bandwith system with normal CP, the sample rate is recommended to be 30.72MHz, and the IDFT size is 2048 accordingly.

A set of sequences is needed to be prepared firstly. Each sequence $q_m(l)$ is based on a distorted $p(l)$ sequence with a CFO f_m which is equally spaced in the searching range of $[-f_{coarse\_\max}, +f_{coarse\_\max}]$ with a certain granularity, and it is expressed by

$$q_m(l) = p(l) \cdot e^{j2\pi \cdot f_m l T_s} \quad . \tag{5}$$

Then for each f_m, correlation can be done according to

$$R^{(m)} = \sum_{l=0}^{N_S-1} y(l) \cdot q_m^{*}(l) = \sum_{l=0}^{N_S-1} y(l) \cdot p^{*}(l) \cdot e^{-j2\pi \cdot f_m l T_S} \quad . \tag{6}$$

where the notation $(\cdot)^*$ means the complex conjugate of its argument; $y(l)$ denotes the received samples of the OFDM symbol with PSS. The coarse frequency error can be estimated by the correlation values comparison according to

$$FOE_{coarse} = \arg\max_{f_m} |R^{(m)}|^2 \quad . \tag{7}$$

So a grid searching of FOE_{coarse} is needed to perform this algorithm. The smaller the searching grid granularity is, the higher the FOE accuracy will be, and the more computational cost is needed. So the granularity can be chosen according to the fine FOE range. And the searching range could be calculated by the minimum requirement about the oscillator stability. For example, as described in [6], the carrier frequency of the BS and UE shall be accurate to within ±0.5ppm and ±2.0ppm observed over a period of one frame respectively, given the carrier frequency of 2.5GHz, the coarse FOE range $f_{coarse\_\max}$ should be 6.25 KHz.

In fine FOE, the phase difference due to the certain gap between PSS symbol and SSS symbol is utilized to estimate the residual CFO. The algorithm runs in the frequency domain. We Let $PSS(k)$ denote the local PSS replica in frequency domain which is a re-ordered $d(n)$ according to

$$PSS(k) = \begin{cases} d(k+30) & k = 1,2...31 \\ d(k-N_s+31) & k = N_s-31,...N_s-1 \\ 0 & others \end{cases} \quad . \tag{8}$$

Denote channel frequency response (CFR) for frequency-time element (k, l_0) as $H(k, l_0)$, i.e. the DFT version of $h(n, l_0)$ defined in (3), the frequency misalignment as Δf, and the initial phase offset as φ_0. Then the received PSS sequence $y_{PSS}(n)$ in the l_0-th OFDM symbol can be represented by

$$y_{PSS}(n) = \frac{1}{N_s} \sum_{k=0}^{N_s-1} PSS(k) H(k, l_0) e^{j2\pi(\frac{nk}{N_s} + \Delta f T_s + \varphi_0)} + \eta_{PSS}(n) \quad . \tag{9}$$

where $n \in [0, N_s - 1]$, η_{PSS} denotes the noise plus interferences from other cells at the receiver. After applying N_s-point DFT, the sequence $Y_{PSS}(k)$ is expressed by

$$Y_{PSS}(k) = PSS(k)H(k,l_0)\frac{\sin(\pi N_s \Delta f T_s)}{N_s \sin(\pi \Delta f T_s)} e^{j\pi(N_s-1)\Delta f T_s + j\varphi_0} + \sum_{m \neq k} I_{k,m}^{PSS} + \eta_{PSS}^{'}(k) \quad . \tag{10}$$

where $\eta_{PSS}^{'}$ denotes the DFT version of η_{PSS}; and $I_{k,m}^{PSS}$ represents the Inter-Carrier Interference (ICI) due to the CFO, which is given by

$$I_{k,m}^{PSS} = PSS(m)H(m,l_0) \bullet \frac{\sin(\pi(m-k-N_s \Delta f T_s))}{N_s \sin(\pi(m-k-N_s \Delta f T_s)/N_s)} e^{-j\pi(1-\frac{1}{N_s})(m-k-N_s \Delta f T_s)+j\varphi_0} \quad . \tag{11}$$

Thus, the product of $Y_{PSS}(k)$ multiplying by $PSS^*(k)$ is given by

$$Y(k) = Y_{PSS}(k)PSS^*(k) = \Theta(k,l_0)e^{j\pi(N_s-1)\Delta f T_s + j\varphi_0} + \eta_{PSS}^{''}(k) \quad . \tag{12}$$

where $\Theta(k,l_0)$ equals to $\frac{\sin(\pi N_s \Delta f T_s)}{N_s \sin(\pi \Delta f T_s)} H(k,l_0)$. The first part of $Y(k)$ is the dominant item carrying the information of Δf, while $\eta_{PSS}^{''}$ is considered to be an interfering part, composed of ICI, noise, and interference.

Similarly, we can also get the sequence $X(k)$ for SSS in the l_1-th OFDM symbol by

$$X(k) = \Theta(k,l_1)e^{j(\pi(N_s-1)\Delta f T_s + \varphi_0 - 2\pi N_{gap} \Delta f T_s)} + \eta_{SSS}^{''}(k) \quad . \tag{13}$$

where N_{gap} denotes the delay from PSS to SSS measured in time samples. As it can be observed from (12) and (13), there is a phase difference proportional to N_{gap} and Δf between dominant part of $X(k)$ and $Y(k)$, so that we can calculate the sequence $Z(k)$ according to

$$Z(k) = Y(k)X^*(k) = \Theta(k,l_0)\Theta^*(k,l_1)e^{j2\pi N_{gap} \Delta f T_s} + \eta^{\sim} \quad . \tag{14}$$

where $k \in [1,31] \cup [N_s - 31, N_s - 1]$ according to the mapping in (8), and the interference $\eta^{\sim}$ is

$$\begin{aligned} \eta^{\sim} \approx\ & \Theta(k,l_0)e^{j\pi(N_s-1)\Delta f T_s + j\varphi_0}\left(\sum_{m \neq k} I_{k,m}^{SSS} + \eta_{SSS}^{'}(k)\right)^* SSS(k) + \\ & \Theta^*(k,l_1)e^{-j\pi(N_s-1)\Delta f T_s - j\varphi_0 + j2\pi N_{gap} \Delta f T_s}\left(\sum_{m \neq k} I_{k,m}^{PSS} + \eta_{PSS}^{'}(k)\right)PSS^*(k) \end{aligned} \quad . \tag{15}$$

Then we can get the FOE_{fine} from the phase of the average of $Z(k)$ as

$$FOE_{fine} = \frac{1}{2\pi N_{gap} T_S} phase\{\frac{1}{N_d}\sum_k Z(k)\} \quad . \tag{16}$$

where N_d denotes the effective length of Z(k), i.e. 62.

From (14) and (15) it can be found that the estimation error comes from 3 factors: ICI ($\sum_{m\neq k} I_{k,m}$), noise and interference from other cells (η'_{PSS}, η'_{SSS}), time variance of the CFR ($H(k,l_0)H^*(k,l_1)$). As a result, the performance would have degradation if the residual frequency error remains still high after coarse FOE. And high vehicular speed, stronger interference and noise could degrade the performance as well. Nevertheless, to compare with conventional CP based method with the same correlation length and system assumptions, the proposed method can combat the multi-path fading effectively because it operates in frequency domain. Moreover, since there are other physical channels mapped to the subcarriers of PSS symbol and SSS symbol, the DFT computations for these symbols which are always required whether the proposed FOE is applied or not, should not be included when evaluating the computational complexity.

3.3 Comparisons between TDD and FDD for the Proposed Fine FOE

In order to compare the performance of the proposed fine FOE in FDD mode with that in TDD mode, the interference $\eta^{\sim}$ in (15) can be regarded as a phase interference $\Delta\theta$ to Z(k), as shown in Fig. 2. Obviously, $\Delta\theta$ is relevant to both magnitude and phase of $\eta^{\sim}$. Here we assume the residual CFO, channel state and carrier to interference plus noise ratio (CINR) are all the same for both modes. Then the only difference in $\eta^{\sim}$ between FDD and TDD is the phase offset of $e^{-j\pi(N_s-1)\Delta fT_s - j\varphi_0 + j2\pi N_{gap}\Delta fT_s}$ as shown in the second part of (15); however the phase of η'_{PSS} rotate randomly, thus the phase offset take little effect on the variance of $\Delta\theta$, and $|\Delta\theta|$ can be weighed mainly dependent on mean magnitude of $\eta^{\sim}$ as

$$mean(|\Delta\theta|) \propto \frac{mean(|\eta^{\sim}|)}{\Phi} \quad . \tag{17}$$

where $\propto$ means a positive relationship; Φ denotes the average magnitude of dominant part of Z(k).

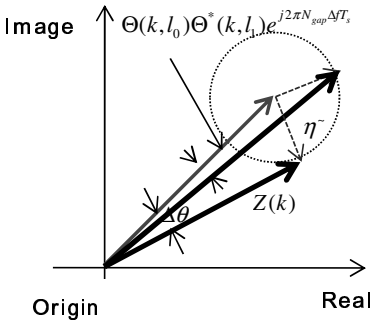

Fig. 2. Estimation error regarded as phase interference

Thus with the same assumptions, the average phase error $|\Delta\theta|$ can be considered almost the same in both FDD and TDD modes, and the fine FOE error Δf_{fine_error} is mainly determined by

$$\Delta f_{fine\_error} \propto \frac{mean(|\tilde{\eta}|)}{N_{gap} T_s \Phi} \quad . \tag{18}$$

Due to that N_{gap} in TDD mode is longer than that in FDD mode; TDD mode can get higher estimation accuracy than FDD mode if the CFO is within both estimation ranges.

On the other hand, considering that the period of complex exponent equals to 2π, according to (14) the estimation range depends on the N_{gap} which differs in FDD and TDD modes, given by

$$\begin{aligned} &|2\pi N_{gap} \Delta f T_s| < \pi \\ &|\Delta f| < \frac{F_s}{2 * N_{gap}} \end{aligned} \quad . \tag{19}$$

For FDD mode, the theoretical searching range is from -7.003 KHz to +7.003 KHz, while it declines to the region of [-2.33KHz, +2.33KHz] for TDD mode. Therefore, we should choose different granularities in coarse FOE for the two modes. For FDD mode, the grid granularity could be 3 KHz as recommended, while for TDD mode, a more accurate coarse FOE is required, e.g. 1 KHz is recommended, otherwise the desired performance cannot to be guaranteed. For low CINR or bad channel state in TDD mode, we need to do extra compensation based on CP [7] to attain the requirement. As a result, TDD mode could estimate the CFO more accurately but need higher computational complexity in coarse FOE.

4 Simulation Results

In order to evaluate the algorithms in a more practical scenario, a multi-cell environment setup is needed. In this paper we simplify the model to a dual-cell scenario to get a revelatory simulation result.

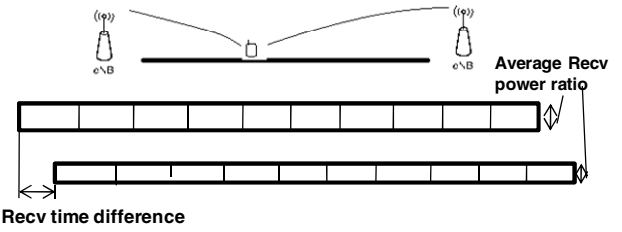

Fig. 3. Dual-cell system model

In the dual-cell scenario, it is assumed that the UE locates on the straight line of the two eNBs, as shown in Fig. 3. The inter-cell distance can be set as 1732 m as recommended in [8]. Besides, the two eNBs are supposed to be strictly synchronous and share the same transmitting carrier frequency. Thus the received time and power differences at UE mainly depend on its distances toward these two eNBs without taking shadowing deviation into account. System parameters are listed in Table I. And the parameters of the transmitter, Okumura-Hata propagation model [9], and the receiver are provided in Table II. One eNB can be selected as the target eNB from which the average received signal power is stronger, and the other is considered as the interfering one. Given the distances from UE to the two eNBs, the system bandwidth, and the RF carrier frequency, the power of the received signal from both eNBs, $P_{t\arg et}$ and $P_{\text{int}erf}$ can be simply calculated without considering the shadowing effect, and the noise power W of the receiver, thus the CINR can be calculated according to

$$CINR = \frac{P_{t\arg et}}{P_{\text{int}erf} + W} \quad . \tag{20}$$

And the performance is to be evaluated based on such a set of practical and reasonable CINR according to (20).

Table 1. System Parameters Description

Parameters	Explanations & Assumptions
Multi-cell Model	Dual-cell
Inter-cell distance	1732 m
Carrier frequency	2.5 GHz
Bandwidth	20 MHz
Antenna Configuration	SISO
Network synchronization	Synchronous

Table 2. Downlink Link Level Parameters

	Parameters	Explanations & Assumptions
eNB Transmitter	Tx Power	43 dBm
	Tx Antenna Gain	14 dBi
	Total Tx Power	57 dBm
Okumura-Hata	BS Antenna Height	15 m
Propagation Model	Distance Dependent Loss	$130.2 + 37.6\lg(r_{km})$
	Fading Channel	ETU 70km/h [10]
	Penetration Loss	20dB
UE receiver	Noise Figure	9 dB
	Thermal noise density	-174 dBm/Hz
	Rx antenna Gain	0 dBi
	Rx noise Effected Power	-92.45 dBm

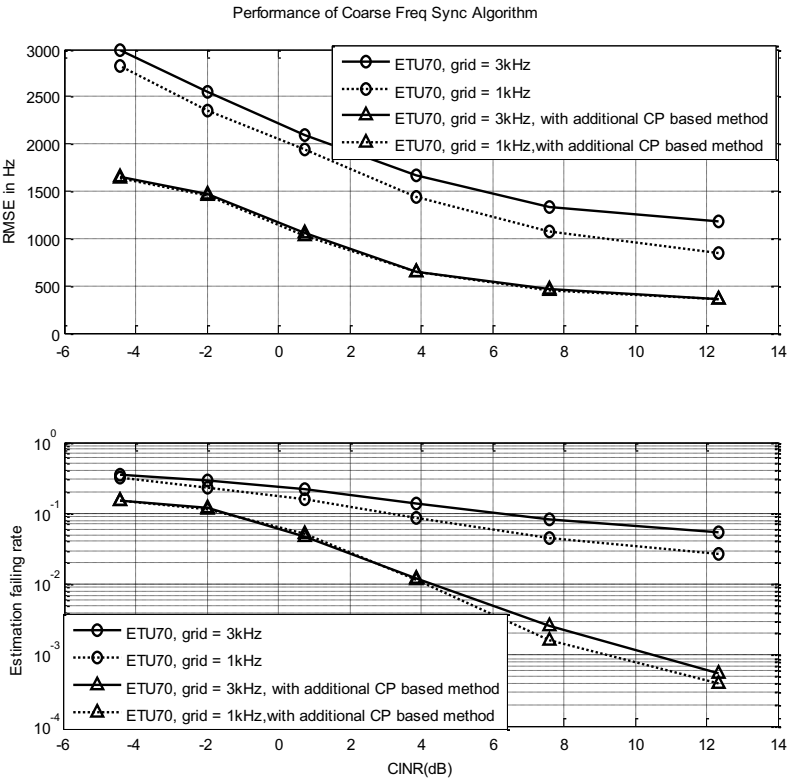

Fig. 4. RMSE and failing rate of coarse frequency synchronization vs. CINR, with grid granularity of 1KHz and 3KHz, searching range of [-9K, 9K], and frequency misalignment uniformly distributed in the searching range.

Fig. 4 shows the performance of coarse FOE in terms of root mean square errors (RMSE) in subplot(a), and failing rate with the threshold of 2 KHz residual frequency error illustrated in subplot(b) respectively. We can see that coarse FOE with 1 KHz grid granularity outperforms the case with 3 KHz granularity. Extra effort based on CP is taken to meet the requirement of fine FOE for TDD mode, whose performance is also illustrated in the figure. With additional CP based method, both the failing rate and RMSE reduce prominently.

In Fig. 5, the RMSE of fine FOE measured in Hz for both FDD and TDD against CINR is illustrated. We consider a frequency misalignment of 1.5K and 1K respectively. From the figure we can see that the residual RMSE of TDD is smaller than that of FDD, with a 4-5dB performance gap. Moreover, we can see that the performance of these two modes is sensitive to the CFO, the larger the original CFO is, the larger residual CFO would be after fine FOE.

The performance of CP based method with autocorrelation length of 62, which is identical in both FDD and TDD modes, is also illustrated in Fig. 5. By comparing the simulation results, we can see that the proposed method has a better performance than CP based method in both modes. In multi-cell environment, the advantage is foreseen to be more apparent because the equivalent multi-path effect becomes much worse which the CP based method is sensitive to.

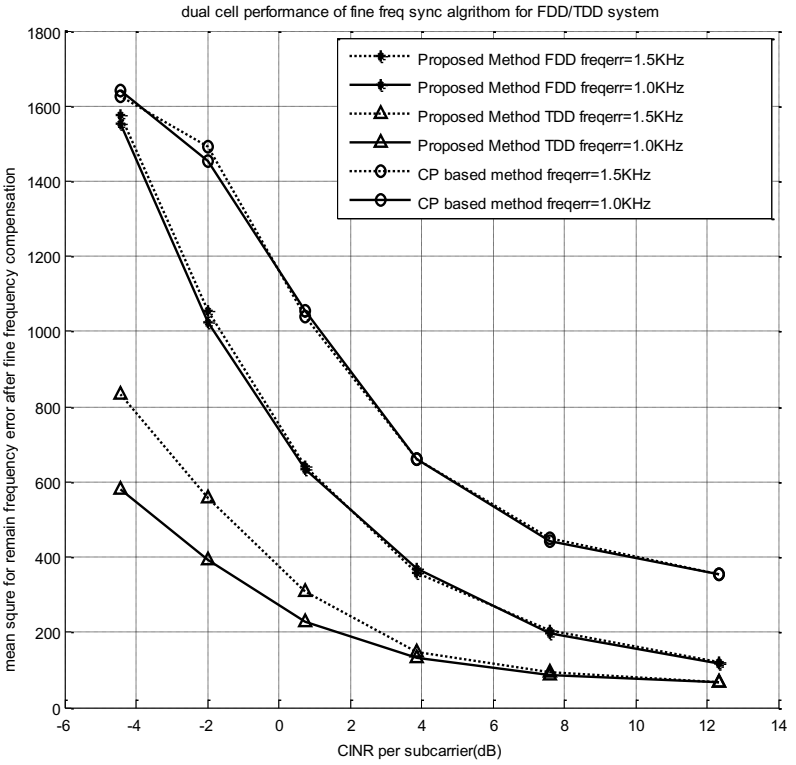

Fig. 5. RMSE of fine frequency synchronization vs. CINR, for both TDD and FDD modes together with CP based method, with assuming frequency errors of 1.5KHz and 1.0KHz.

5 Conclusion

In this paper, we propose a new frequency synchronization method based on synchronization signals including coarse FOE and fine FOE for both FDD and TDD modes. To compare with traditional CP based method, the proposed fine FOE can estimate the CFO more accurately, especially in the practical multi-cell environment. In addition, both the mathematical analysis and the comparison results show that the proposed fine FOE in TDD has higher estimation accuracy but needs more computational cost in coarse FOE than that in FDD.

References

1. Holma, H., Toskala, A.: LTE for UMTS- OFDMA and SC-FDMA Based Radio Acess, pp. 2–22. John Wiley & Sons (2009)
2. Manolakis, K., Gutierrez Estevez, D.M., Jungnickel, V., Wen, X., Drewes, C.: A Closed Concept for Synchronization and Cell Search in 3GPP LTE Systems. In: IEEE Wireless Communications and Networking Conference (2009)
3. Tsai, P.-Y., Chang, H.-W.: A new cell search scheme in 3GPP long term evolution downlink, OFDMA systems. IEEE Wireless Communications & Signal Processing (April 2009)
4. Shim, M.J., Han, J.S., Roh, H.J., Choi, H.J.: A frequency synchronization method for 3GPP LTE OFDMA system in TDD mode. IEEE Communications and Information Technology (2009)
5. 3GPP TS 36.211 V9.1.0, Physical channels and modulation (March 2010)
6. 3GPP TS 36.101 V9.1.0, User Equipment (UE) radio transmission and reception (September 2009)
7. Sandell, M., van de Beek, J.J., Börjesson, P.O.: Timing and Frequency Synchronization in OFDM Systems Using the Cyclic Prefix. In: Proc. IEEE Int. Symp. Synchronization, Essen, Germany (December 1995)
8. ITU Publications, Guidelines for evaluation of radio interface technologies for IMT-Advanced, ITU-R Reports M.2135 (2008)
9. Hata, M.: Empirical formula for propagation loss in land mobile radio services. IEEE Transactions on Vehicular Technology, 29(3) (1980)
10. 3GPP TS 36.141 V8.8.0, Base Station (BS) conformance testing (September 2010)